The Journal of Immunology

Metabolic Reprogramming Commits Differentiation of Human CD27 $^{+}$IgD^{+} B Cells to Plasmablasts or CD27^{-}IgD^{-} Cells

Masataka Torigoe, Shigeru Iwata, Shingo Nakayamada, Kei Sakata, Mingzeng Zhang, Maiko Hajime, Yusuke Miyazaki, Manabu Narisawa, Koji Ishii, Hirotaka Shibata and Yoshiya Tanaka

J Immunol 2017; 199:425-434; Prepublished online 16 June 2017;
doi: 10.4049/jimmunol.1601908
http://www.jimmunol.org/content/199/2/425

The Journal of Immunology is published twice each month by
The American Association of Immunologists, Inc.,
1451 Rockville Pike, Suite 650, Rockville, MD 20852

Print ISSN: 0022-1767 Online ISSN: 1550-6606.

Metabolic Reprogramming Commits Differentiation of Human CD27$^+$IgD$^+$ B Cells to Plasmablasts or CD27$^-$IgD$^-$ Cells

Masataka Torigoe,*,† Shigeru Iwata,* Shingo Nakayamada,* Kei Sakata,*,‡ Mingzeng Zhang,* Maiko Hajime,* Yusuke Miyazaki,* Manabu Narisawa,* Koji Ishii,† Hirotaka Shibata,† and Yoshiya Tanaka*

B cells play a crucial role in the pathogenesis of autoimmune diseases, such as systemic lupus erythematosus (SLE). However, the relevance of the metabolic pathway in the differentiation of human B cell subsets remains unknown. In this article, we show that the combination of CpG/TLR9 and IFN-α markedly induced the differentiation of CD27$^+$IgD$^+$ unswitched memory B cells into CD27^{hi} CD38^{hi} plasmablasts. The response was accompanied by mammalian target of rapamycin complex 1 (mTORC1) activation and increased lactate production, indicating a shift to glycolysis. However, CpG alone induced the differentiation of unswitched memory B cells into CD27$^-$IgD$^-$ memory B cells with high cytokine production, but such differentiation was suppressed by IFN-α. AMP-activated protein kinase activation enhanced the differentiation to CD27$^-$IgD$^-$ B cells, but it attenuated mTORC1 activation and differentiation into plasmablasts. High mTORC1 activation was noted in CD19$^+$ B cells of patients with SLE and correlated with plasmablast differentiation and disease activity. Taken together, differential metabolic reprogramming commits the differentiation of human unswitched memory B cells into plasmablasts (the combination of CpG and IFN-α amplifies mTORC1-glycolysis pathways) or CD27$^-$IgD$^-$ memory B cells (CpG alone amplifies the AMP-activated protein kinase pathway). The former metabolic pathway may play a pivotal role in SLE. ***The Journal of Immunology*****, 2017, 199: 425–434.**

B cells produce Abs and control the immune system through cytokine production and Ag presentation. Recent studies demonstrated that TLRs, which are involved in innate immunity, enhance the immune responses of B cells. TLR9 recognizes CpG-DNA derived from bacteria and viruses and is expressed on B cells and plasmacytoid dendritic cells (1). TLR9 signal induces plasmablast differentiation, cytokine production, and expression of costimulatory molecules of B cells (2–5). With regard to plasmacytoid dendritic cells, the TLR9 signal promotes their Ag presentation and IFN-α production (6). IFN-α promotes B cell survival, class switch recombination, and Ig production (7, 8). B cell activation by TLR9 and IFN-α contributes to Ag removal in infections and plays a role in the pathogenesis of various autoimmune diseases, such as systemic lupus erythematosus (SLE) (9).

CD19$^+$ B cells are classified into three subsets based on CD27 and IgD expression: naive B cells (CD27$^-$IgD$^+$), unswitched memory B cells (CD27$^+$IgD$^+$), and class-switched memory B cells (CD27$^+$IgD$^-$). In particular, the nature of unswitched memory B cells remains to be defined. Some reports (10–12) suggested that these cells are the circulating marginal zone B cells formed independently of the germinal center response. They carry a somatic hypermutation, although they do not go through class switch recombination. The first-line defense strategy, through rapid production of low-affinity, but high-avidity, IgM upon pathogen challenge, is a unique feature of this subset (11, 13, 14). How B cell subsets exhibit effector functions and differentiate into plasmablasts or a long-lived memory phenotype remain unknown (15).

We previously reported the presence of significantly higher percentages of plasmablasts and CD27$^-$IgD$^-$ memory B cells and a significantly lower percentage of CD27$^+$IgD$^+$ memory B cells in the peripheral blood of SLE patients compared with control subjects (5). In addition, the number and percentages of CD27^{hi} plasmablasts correlated significantly with indices of SLE disease activity and with the titer of anti-dsDNA autoantibodies. However, the mechanism of increment in plasmablasts and CD27$^-$IgD$^-$ memory B cells in SLE patients remains unclear.

Activation and differentiation of effector T cells depend on rapid synthesis of cell structure components and biomolecules, therefore demanding enormous amounts of energy, nucleic acids, lipids, and amino acids (16). Recent studies demonstrated that the metabolic

*First Department of Internal Medicine, School of Medicine, University of Occupational and Environmental Health, Japan, Kitakyushu, Fukuoka 807-8555, Japan; †Department of Endocrinology, Metabolism, Rheumatology and Nephrology, Faculty of Medicine, Oita University, Yufu, Oita 879-5593, Japan; and ‡Mitsubishi Tanabe Pharma, Yokohama, Kanagawa 227-0033, Japan

Received for publication November 8, 2016. Accepted for publication May 18, 2017.

This work was supported in part by Grants-In-Aid for Scientific Research from the Ministry of Education, Culture, Sports, Science and Technology of Japan (Grants 22249025 and 16K09928), the Ministry of Health, Labor and Welfare of Japan (Grant H26-008), the Japan Agency for Medical Research and Development (Grant 16ek0410016h0003), and the University of Occupational and Environmental Health, Japan through a grant for advanced research (Grant H23-Q-916).

M.T., S.I., and S.N. designed the study; M.T. conducted the experiments, analyzed the data, and wrote the manuscript; K.S., M.Z., M.H., Y.M., and M.N. helped to conduct the experiments; K.I. and H.S. supervised the research; and Y.T. created the research concept and supervised the research and writing of the manuscript.

Address correspondence and reprint requests to Prof. Yoshiya Tanaka, First Department of Internal Medicine, School of Medicine, University of Occupational and Environmental Health, Japan, 1-1 Iseigaoka, Yahata-nishi, Kitakyushu, Fukuoka 807-8555, Japan. E-mail address: tanaka@med.uoeh-u.ac.jp

The online version of this article contains supplemental material.

Abbreviations used in this article: AICAR, 5-aminoimidazole-4-carboxamide ribonucleotide; AMPK, AMP-activated protein kinase; 2-DG, 2-deoxy-D-glucose; MFI, mean fluorescence intensity; mTORC1, mammalian target of rapamycin complex 1; p-S6, phosphorylated ribosomal S6 protein; SLE, systemic lupus erythematosus.

shift to anabolism, including aerobic glycolysis, is also necessary for the activation of various types of murine immune cells (17–19). It has been reported that the mammalian target of rapamycin complex 1 (mTORC1) accelerates a metabolic shift to glycolysis in activated $CD4^+$ T cells and $CD8^+$ T cells (20, 21). mTORC1 is activated by specific stimulants, including cytokines, growth factors, and nutrients. Downstream, it enhances mRNA translation and ribosome biogenesis, while suppressing such catabolic processes as fatty acid oxidation and oxidative phosphorylation in the mitochondria (22, 23), which efficiently produce ATP (24). AMP-activated protein kinase (AMPK) promotes oxidative phosphorylation but indirectly suppresses the mTORC1 pathway via sensing glucose deprivation. Briefly, AMPK converts anabolism to catabolism (25). Thus, although metabolic reprogramming is important for the activation of various human immune cells and murine B cells (26, 27), human B cells have been studied minimally in this context.

The present study was designed to determine the effects of TLR9 and/or IFN-α signal on the functions and differentiation of each human B cell subset. The results demonstrated the relevance of cellular metabolic changes in the differentiation of human B cell subsets.

Materials and Methods

Reagents

Rapamycin was purchased from Selleck Chemicals (Houston, TX); metformin hydrochloride, 5-aminoimidazole-4-carboxamide ribonucleotide (AICAR), hydroxychloroquine sulfate, and active human IFN-α full-length protein were from Abcam (Cambridge, MA); anti-human IFNAR2 Ab was from PBL Assay Science (Piscataway, NJ); 2-deoxy-D-glucose (2-DG) was from Wako Pure Chemical Industries (Osaka, Japan); and CpG oligonucleotide 2006 and loxoribine were purchased from InvivoGen (San Diego, CA).

Isolation, culture, and stimulation of B cell subsets

PBMCs were isolated from healthy adults with lymphocyte separation medium (Lympholyte-H; CEDARLANE, Burlington, NC) and treated with magnetic beads (Dynabeads CD19 pan B; Thermo Fisher Scientific, Waltham, MA). $CD19^+$ B cell purity was >98%, as determined by flow cytometric analysis. The purified $CD19^+$ B cells (2×10^5 cells per 200 μl) were cultured alone or with 1000 U/ml IFN-α, 0.5 μM CpG-ODN, 1 mM loxoribine, and/or reagents. B cell sorting was performed on a FACSAria II (BD Biosciences, San Jose, CA). For isolation of human $CD27^-IgD^+$ naive B cells, $CD27^+IgD^+$ unswitched memory B cells, and $CD27^+IgD^-$ class-switched memory B cells, the purified $CD19^+$ B cells were stained with anti-CD27 and anti-IgD Abs. Each subset of B cells (0.5×10^5 cells per 200 μl) was cultured alone or with the aforementioned stimulation and/or treatment. The culture medium was RPMI 1640 (Wako Pure Clinical Industries) supplemented with 10% FCS (Tissue Culture Biologicals, Tulare, CA), 100 U/ml penicillin, and 100 U/ml streptomycin (Thermo Fisher Scientific).

Patients

PBMCs were obtained from 48 patients with SLE and 16 healthy donors. The clinical characteristics of the subjects are detailed in Table I. For flow cytometric analysis, PBMCs were stained with anti-CD19 Ab and anti–p-mTOR Ab by intracellular staining. Then, CD19-gated cells were analyzed for p-mTOR expression. The study, including the collection of peripheral blood samples from healthy adults and patients, was approved by the Human Ethics Review Committee of the University of Occupational and Environmental Health, Japan. Each subject provided a signed consent form.

Flow cytometric analysis

After washing, B cells were incubated in blocking buffer (0.25% human globulin, 0.5% human albumin [Mitsubishi Tanabe Pharma, Osaka, Japan], and 0.1% NaN_3 in PBS) in a 96-well plate at 4°C for 15 min. Cells were then suspended in 100 μl of FACS solution (0.5% human albumin and 0.1% NaN_3 in PBS) and stained with the following fluorochrome-conjugated anti-human Abs: anti-CD19 (HIB19), anti-IgD (IA6-2), anti-IgG (G18-145), anti-IgM (G20-127), anti-CD27 (M-T271), anti-CD38 (HIT2), anti-CD80 (16-10A1), anti-CD86 (FUN-1), anti-CD95 (DX2), anti–HIF-1α (54/HIF-1α), anti-S6 (pS235/pS236) (N7-548), anti-mTOR (pS2448) (O21-404), anti-Ki-67 (B56), and isotype-matched mouse IgG controls (all from BD Biosciences) for 30 min at 4°C. To exclusively analyze live populations, these cells were also stained with propidium iodide (BD Biosciences). For intracellular staining, the cells were first fixed and permeabilized with a Transcription Factor Buffer Set (BD Biosciences), washed three times with FACS solution, and analyzed with FACSVerse (BD Biosciences)/FlowJo software (TOMY Digital Biology, Tokyo, Japan).

Cytokine production

The levels of IL-6, IL-10, and TNF-α in the culture medium were determined using a BD Cytometric Bead Array (CBA) Human Flex Set (BD Biosciences), according to the instructions supplied by the manufacturer.

ELISA for IgM and IgG

For quantification of in vitro IgG and IgM secretion, B cells were cultured alone or under stimulation/treatment in 96-well plates for 5 d. IgM and IgG levels in the culture medium were determined by using a Human IgG/IgM ELISA Quantitation Set (Bethyl Laboratories, Montgomery, TX), according to the protocol provided by the manufacturer.

Quantitative real-time PCR

Total RNA was extracted using an RNeasy Mini Kit (QIAGEN, Valencia, CA). First-strand cDNA was synthesized, and quantitative real-time PCR was performed using a StepOnePlus instrument (Applied Biosystems, Waltham, MA) in triplicate wells in 96-well plates. The TaqMan target mixes for BCL6 (Hs00153368_m1), BACH2 (Hs00222364_m1), IRF4 (Hs01056533_m1), PRDM1 (Hs00153357_m1) and XBP-1 (Hs00152973-m1) were purchased from Applied Biosystems. The expression level of each mRNA was normalized to the level of the endogenous control 18S rRNA (Hs99999901_m1; Applied Biosystems).

Lactate assay

B cells were cultured alone or under stimulation/treatment for 5 d in 96-well plates. The culture medium was collected and diluted properly for measurement of lactate concentration using a Lactate Assay Kit II (BioVision, Milpitas, CA) and the protocol supplied by the manufacturer.

Cell viability assay

B cells were cultured alone or under stimulation for 5 d in 96-well plates. After culture, the cells were suspended in 100 μl of FACS solution and stained with propidium iodide. The percentage of living cells was measured by flow cytometry.

Statistical analysis

Differences between groups were examined for statistical significance by the paired *t* test. A p value <0.05 was considered statistically significant. Statistical analyses were conducted using Prism software (Prism Software, Irvine, CA)

Results

CpG/TLR9 and IFN-α–enhanced differentiation of human B cells

We first investigated the effects of TLR9 and/or IFN-α signal on the differentiation of human $CD19^+$ B cells into plasmablasts. Human $CD19^+$ B cells were cultured for 5 d alone or with CpG (TLR9 ligand) and/or IFN-α. $CD27^{hi}$ cells were robustly induced by CpG but not by IFN-α alone. The proportion of $CD27^{hi}$ plasmablasts was further increased by the combination of CpG and IFN-α, and these cells highly expressed CD38, indicating they were plasmablasts (Fig. 1A). Next, CpG induced the secretion of IgG and IgM, and this effect was amplified by the addition of IFN-α (Fig. 1B). Furthermore, the combination of CpG and IFN-α induced strong expression of IRF4, PRDM1, and XBP1 but suppressed BCL6 and BACH2 (Fig. 1C). These results suggest that CpG/TLR9-signal drives human B cell differentiation to $CD27^{hi}$ cells and that IFN-α signal amplifies CpG-induced differentiation and facilitates the development of $CD27^{hi}CD38^{hi}$ plasmablasts with high Ig-production capacity.

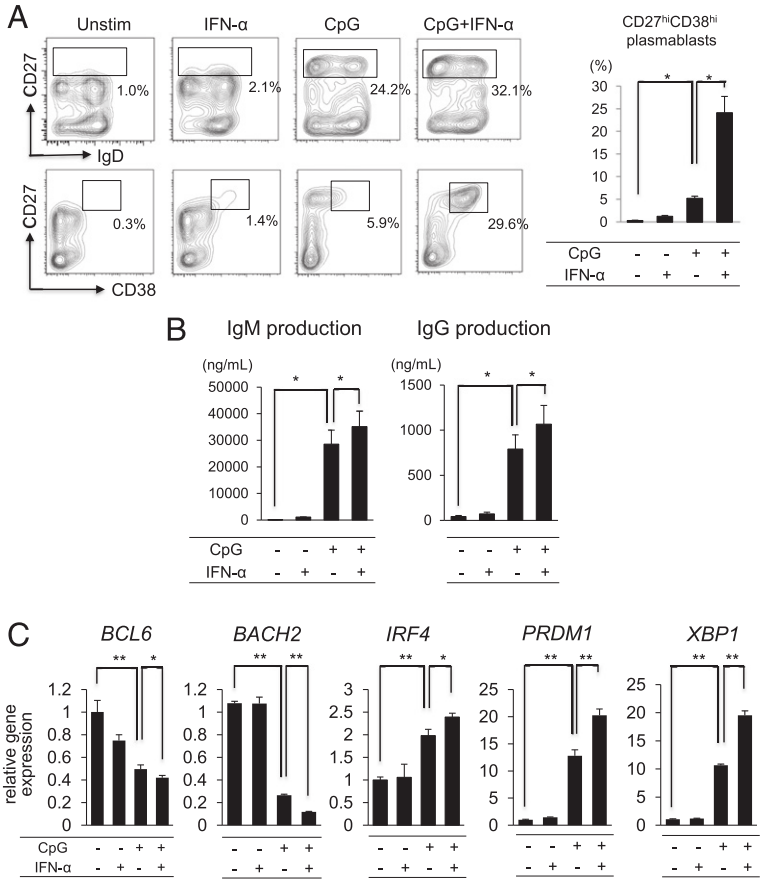

FIGURE 1. CpG/TLR9 induced robust immune functions of human B cells, which were further augmented by IFN-α. $CD19^+$ B cells were cultured for 5 d alone, with CpG/TLR9, or with IFN-α. (**A**) Surface expression of CD27, IgD, and CD38 was analyzed by flow cytometry to evaluate plasmablast differentiation and maturation after stimulation. (**B**) IgM and IgG production was quantified by ELISA. (**C**) Gene expression of transcription factors for B cell differentiation was assessed by RT-PCR. Contour plots are representative of three independent experiments that yielded the same results. Data are mean ± SEM of three independent experiments using cells from three different donors. $*p < 0.05$, $**p < 0.01$.

CpG induces $CD27^-IgD^-$ memory B cells and CpG+IFN-α induces $CD27^{hi}CD38^{hi}$ plasmablasts from unswitched memory B cells

Peripheral human $CD19^+$ B cells were divided into three subsets based on the stage of differentiation: naive B cells ($CD27^-IgD^+$), unswitched memory B cells ($CD27^+IgD^+$), and class-switched memory B cells ($CD27^+IgD^-$). Next, we evaluated the responses of these three B cell subsets to TLR9 and/or IFN-α stimulation. The purity of each subset was >95% (Fig. 2A).

When stimulated with CpG, $CD27^+IgD^+$ and $CD27^+IgD^-$ memory B cells, but not $CD27^-IgD^+$ naive B cells, exhibited equivalently efficient differentiation into $CD27^{hi}$ B cells. Membrane IgD, similar to IgM and IgG, is known to function as a BCR (28). Because stimulation with CpG does not induce BCR cross-linking, which leads to class switch recombination (29), some of the plasmablasts from $CD27^+IgD^+$ memory B cells continued to express IgD (Fig. 2). CpG also characteristically induced $CD27^-IgD^-$ memory B cells, primarily from $CD27^+IgD^+$ unswitched memory B cells. TLR7 ligand LOX did not induce $CD27^-IgD^-$ memory B cells (Supplemental Fig. 1D). The addition of IFN-α reduced the proportion of CpG-induced $CD27^-IgD^-$ B cells (Fig. 2A). In contrast, the addition of IFN-α and CpG to the $CD27^+$ memory B cell subsets markedly induced their differentiation into $CD27^{hi}IgD^-$ plasmablasts with high expression of CD38 (Fig. 2A). The increment in $CD27^{hi}CD38^{hi}$ well-differentiated plasmablast formation by CpG+IFN-α was reversed to the baseline level by anti-IFNAR2 Ab (Fig. 2B).

Next, we evaluated the cell proliferation and rate of apoptosis, using Ki-67 and propidium iodide staining, respectively, of the three B cell subsets stimulated with CpG and/or IFN-α. Proliferation of the $CD27^+$ memory B cell subsets (represented by Ki-67 expression) was robustly induced by CpG and synergistically amplified by IFN-α (Supplemental Fig. 1A, 1B). In contrast, the extent of apoptosis was similar in all three subsets, irrespective of stimulation with CpG, IFN-α, or their combinations (Supplemental Fig. 1C). These results suggest that plasmablast differentiation seems to depend on the proliferative potential of B cell subsets. This conclusion was also based on the previous finding linking plasmablast differentiation to B cell division (30).

These results suggest that $CD27^+IgD^+$ memory B cells efficiently differentiate into $CD27^-IgD^-$ B cells, as well as $CD27^{hi}$ B cells, in response to CpG/TLR9 signal. The combination of CpG and IFN-α promoted differentiation into $CD27^{hi}CD38^{hi}$ plasmablasts and suppressed the transition to $CD27^-IgD^-$ B cells by these memory B cells.

CpG+IFN-α induces the greatest production of Ig and cytokines from $CD27^+IgD^+$ unswitched memory B cells

In the next step, the Ig-production capacity of each of the three subsets was analyzed. The capacity for Ig production was extremely poor in $CD27^-IgD^+$ naive B cells. In contrast, CpG-stimulated $CD27^+IgD^+$ unswitched memory B cells secreted large amounts of IgM, and $CD27^+IgD^-$ class-switched memory B cells produced large amounts of IgG. These activities were amplified by the addition of IFN-α (Fig. 3A). Cytokine production was greatest by unswitched memory B cells. Furthermore, the addition of IFN-α augmented IL-6 production, but not IL-10 or TNF-α, in unswitched memory B cells and class-switched memory B cells (Fig. 3B). Thus, stimulation of unswitched memory B cells by CpG and/or IFN-α resulted in the most robust production of Ig and cytokines and their differentiation into plasmablasts and $CD27^-IgD^-$ B cells (Fig. 2A). Based on these findings, the following experiments primarily used unswitched memory B cells.

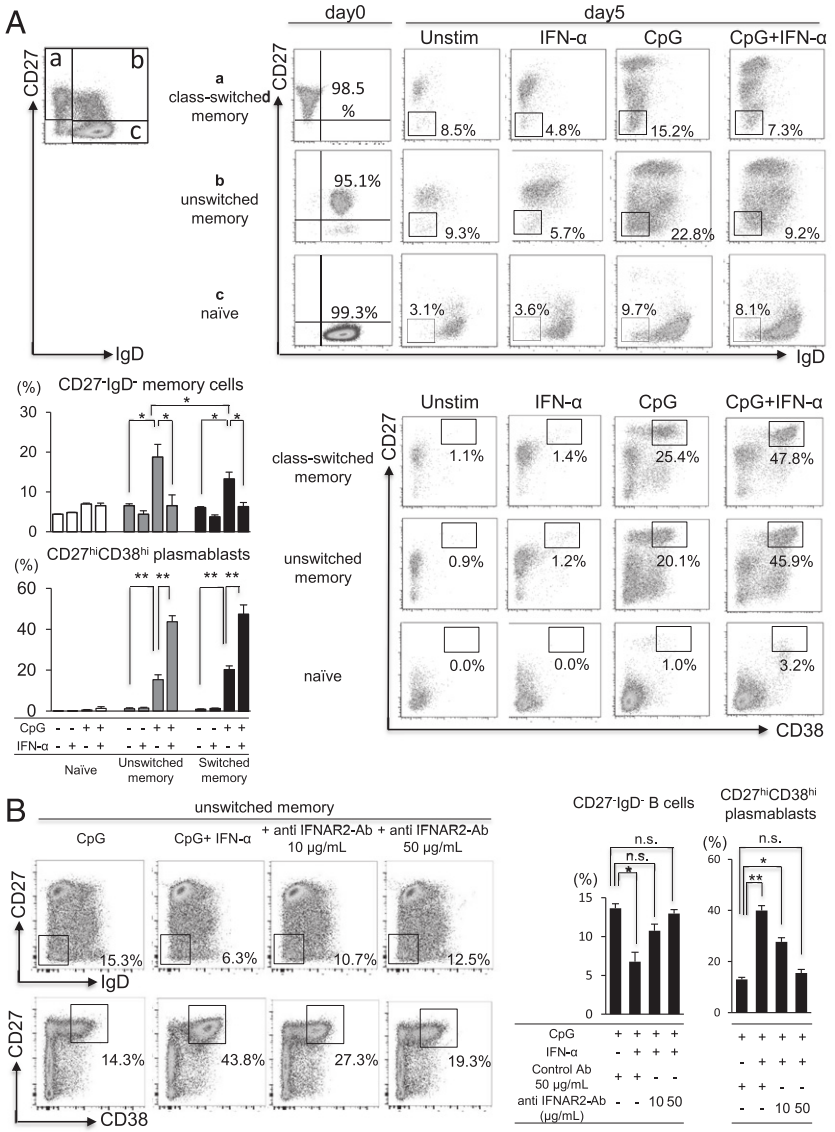

FIGURE 2. $CD27^+IgD^+$ unswitched memory B cells efficiently differentiated into plasmablasts and $CD27^-IgD^-$ B cells through CpG and/or IFN-α. $CD19^+$ total B cells were sorted into three subsets: $CD27^-IgD^+$ naive B cells, $CD27^+IgD^+$ unswitched memory B cells, and $CD27^+IgD^-$ class-switched memory B cells. The three subsets were cultured for 5 d under stimulation. Postsort reanalysis was performed to confirm their purity. (**A**) Expression of surface markers on each B cell subset was assessed by flow cytometry. The percentages of $CD27^-IgD^-$ B cells and $CD27^{hi}CD38^{hi}$ plasmablasts were calculated. (**B**) $CD27^+IgD^+$ unswitched memory B cells were cultured under CpG and IFN-α conditions, with or without anti–IFNAR2-Ab. Data are percentages of plasmablasts and $CD27^-IgD^-$ B cells. Dot plots are representative of three or more independent experiments yielding the same results. Data are mean ± SEM of three experiments using cells from three donors. $*p < 0.05$, $**p < 0.01$.

CpG+IFN-α enhances the mTORC1–glycolysis pathway in the differentiation of unswitched memory B cells into plasmablasts

Next, we examined the cellular metabolic changes to understand the mechanism by which CpG and IFN-α induced differentiation of human B cell subsets. First, we compared CpG-induced phosphorylated ribosomal S6 protein (p-S6), a surrogate of mTORC1 activation, in the three B cell subsets. CpG activated the mTORC1 pathway, especially in unswitched memory B cells and class-switched memory B cells, but to a lesser extent in naive B cells (Fig. 4A). The addition of IFN-α to CpG resulted in robust activation of mTORC1 in unswitched memory B cells (Fig. 4B). Next, we examined lactate production. The combination of CpG and IFN-α significantly induced lactate production, which reflects glycolysis, in unswitched memory B cells (Fig. 4C). Furthermore, the combination of CpG and IFN-α markedly induced $CD27^{hi}CD38^{hi}$ plasmablasts and IgM production in unswitched memory B cells, but treatment of these cells with rapamycin, an mTORC1 inhibitor, and 2-DG, a glycolytic inhibitor, suppressed their differentiation into $CD27^{hi}CD38^{hi}$ plasmablasts and IgM production in a dose-dependent manner (Fig. 4D). Neither rapamycin nor 2-DG altered cell viability when used at the concentrations shown in Fig. 4D (data not shown). Rapamycin and 2-DG also exhibited similar inhibitory effects on plasmablast differentiation and IgG production in CpG and IFN-α–stimulated class-switched memory B cells (Supplemental Fig. 2). These results suggest that CpG/TLR9 and IFN-α signal enhance mTORC1 activation and glycolysis, resulting in differentiation of $CD27^+$ memory B cells into $CD27^{hi}CD38^{hi}$ plasmablasts.

AMPK activation prevents differentiation of unswitched memory B cells to plasmablasts but supports their transition to $CD27^-IgD^-$ B cells

AMPK promotes ATP production through catabolic processes, such as oxidative phosphorylation, but it indirectly suppresses the mTORC1 pathway via sensing glucose deprivation and reduces ATP consumption (24). We next investigated the effects of the AMPK pathway on B cell metabolism and immune responses, using the AMPK activators metformin and AICAR (31, 32). Because $CD27^+IgD^+$ memory B cells have a unique differentiation capacity for plasmablasts, as well as $CD27^-IgD^-$ B cells, compared with $CD27^+IgD^-$ memory B cells (Fig. 2A), we focused on this subset in the investigation of the role of AMPK in B cell differentiation. The AMPK pathway suppressed CpG-induced mTORC1 activation and lactate production, resulting in inhibition of the differentiation of unswitched memory B cells to plasmablasts and suppression of IgM production, but it increased the

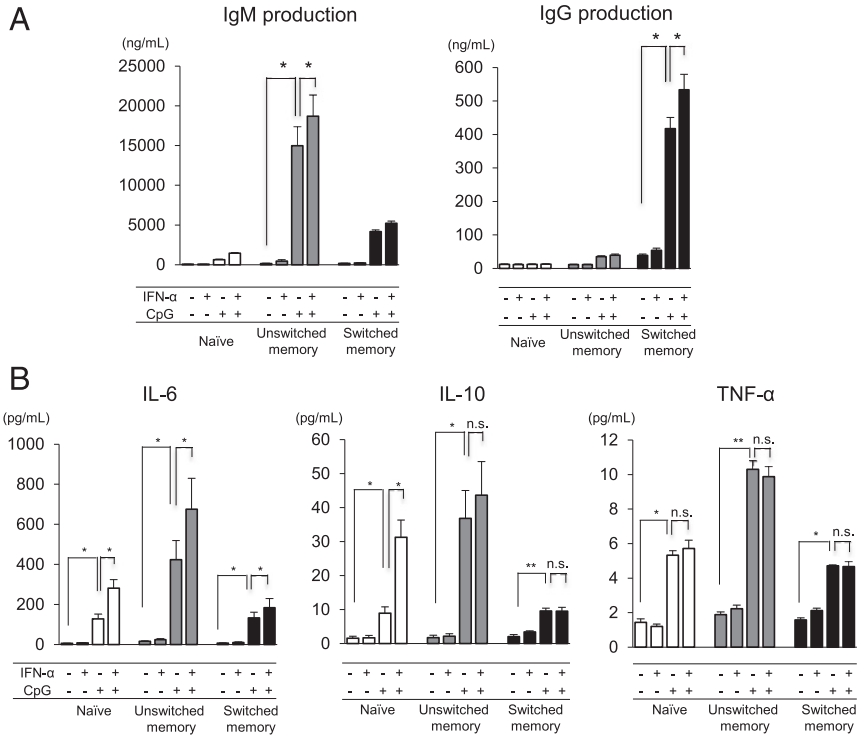

FIGURE 3. $CD27^+IgD^+$ unswitched memory B cells exhibited the most potent effector properties with the largest production of Ig and cytokines. Each B cell subset was cultured with CpG and/or IFN-α for 5 d and analyzed for cytokine and Ig production. (**A**) Production of IgM and IgG by each B cell subset was quantitated by ELISA. (**B**) IL-6, IL-10, and TNF-α concentration was quantified by cytometric bead array. Data are mean ± SEM of three experiments using cells from three donors. $*p < 0.05$, $**p < 0.01$.

proportion of $CD27^-IgD^-$ B cells (Fig. 5A–D). AMPK activators efficiently attenuated plasmablast differentiation, IgM production, and proliferation induced by CpG and IFN-α in $CD27^+IgD^+$ memory B cells, as well as rapamycin and 2-DG (Supplemental Fig. 3A–C). In addition, we investigated the expression of HIF-1α, a transcription factor that promotes glycolysis, by upregulating glucose transporters and glycolytic enzymes (33). In our experiments, CpG induced HIF-1α expression, and the expression level was attenuated by metformin but not AICAR (Fig. 5E). This may account for the more potent suppression of glycolysis, plasmablast differentiation, and Ig production by metformin compared with AICAR.

Next, we assessed p-S6 and several surface markers for more specific characterization of $CD27^-IgD^-$ B cells. CpG-induced $CD27^-IgD^-$ B cells did not express p-S6 (Fig. 5F). Initially, we considered that inhibition of mTORC1 or glycolysis could facilitate the transition to $CD27^-IgD^-$ B cells. However, neither rapamycin nor 2-DG increased the percentage of $CD27^-IgD^-$ B cells (Supplemental Fig. 3D). These data indicate that the transition to $CD27^-IgD^-$ B cells critically depends on inhibition of the mTORC1–glycolysis pathway and activation of AMPK. These results suggest the involvement of the AMPK pathway in the differentiation of unswitched memory B cells to $CD27^-IgD^-$ B cells, whereas the same pathway attenuates mTORC1 activity and glycolysis, as well as the differentiation of unswitched memory B cells into plasmablasts.

We also detected high expression levels of CD80 and CD86, which act as costimulatory molecules, and CD95, a marker of cell activation, in $CD27^-IgD^-$ B cells (Fig. 5F). CpG maintained the expression of membrane IgM, reduced IgD, and did not induce IgG on $CD27^-IgD^-$ B cells derived from $CD27^+IgD^+$ memory B cells (Supplemental Fig. 3E). These results indicate the functionality of $CD27^-IgD^-$ B cells.

Taken together, it seems likely that differential metabolic reprogramming commits the differentiation of human unswitched memory B cells to plasmablasts (CpG and IFN-α–mTORC1 pathway) or $CD27^-IgD^-$ cells (CpG alone–AMPK pathway).

mTORC1 phosphorylation in $CD19^+$ B cells correlates with SLE pathogenesis

Our results demonstrated that CpG and IFN-α, which are critical inflammatory mediators in the pathogenesis of SLE, induced mTORC1 activation and glycolysis in human B cells and resulted in their differentiation into plasmablasts. We next assessed the relevance of mTORC1 activity in SLE. For this purpose, we measured p-mTOR (serine 2448) levels in $CD19^+$ B cells from 48 patients with SLE and 16 healthy donors. Both p-mTOR at serine 2448 and p-S6 specifically reflect mTORC1 activation (34). In our preliminary experiments, anti–p-mTOR at serine 2448 Abs exhibited slightly greater sensitivity and seemed suitable for the detection of differences in the mean fluorescence intensity (MFI) in B cells of healthy subjects and patients with SLE. Therefore, we used anti–p-mTOR at serine 2448 Abs for analysis of patients' samples. Table I summarizes the clinical characteristics of the subjects. The level of p-mTOR in $CD19^+$ B cells was significantly higher in SLE patients compared with healthy subjects (mean ± SD of ΔMFI of p-mTOR in $CD19^+$ B cells: healthy subjects, 533 ± 120; SLE, 962 ± 417, $p < 0.001$) (Fig. 6A). The level of p-mTOR in $CD19^+$ B cells correlated positively with the proportion of peripheral plasmablasts among $CD19^+$ B cells, SLE disease activity index score, and anti-dsDNA Ab titer (Fig. 6B). These results suggest that mTORC1 activation in $CD19^+$ B cells is closely related to plasmablast differentiation and disease activity in patients with SLE.

Discussion

In this study, we found that the combination of CpG/TLR9 and IFN-α stimulates the differentiation of $CD27^+IgD^+$ unswitched memory B cells into plasmablasts and the production of large amounts of Ig and cytokines. In contrast, CpG alone induced $CD27^-IgD^-$ memory B cells with high cytokine production from unswitched memory B cells, but their differentiation was suppressed by IFN-α. Differentiation of unswitched memory B cells into plasmablasts requires metabolic conversion to anabolism with enhanced mTORC1 activation and glycolysis. Conversely, the AMPK pathway enhanced the transition of unswitched memory

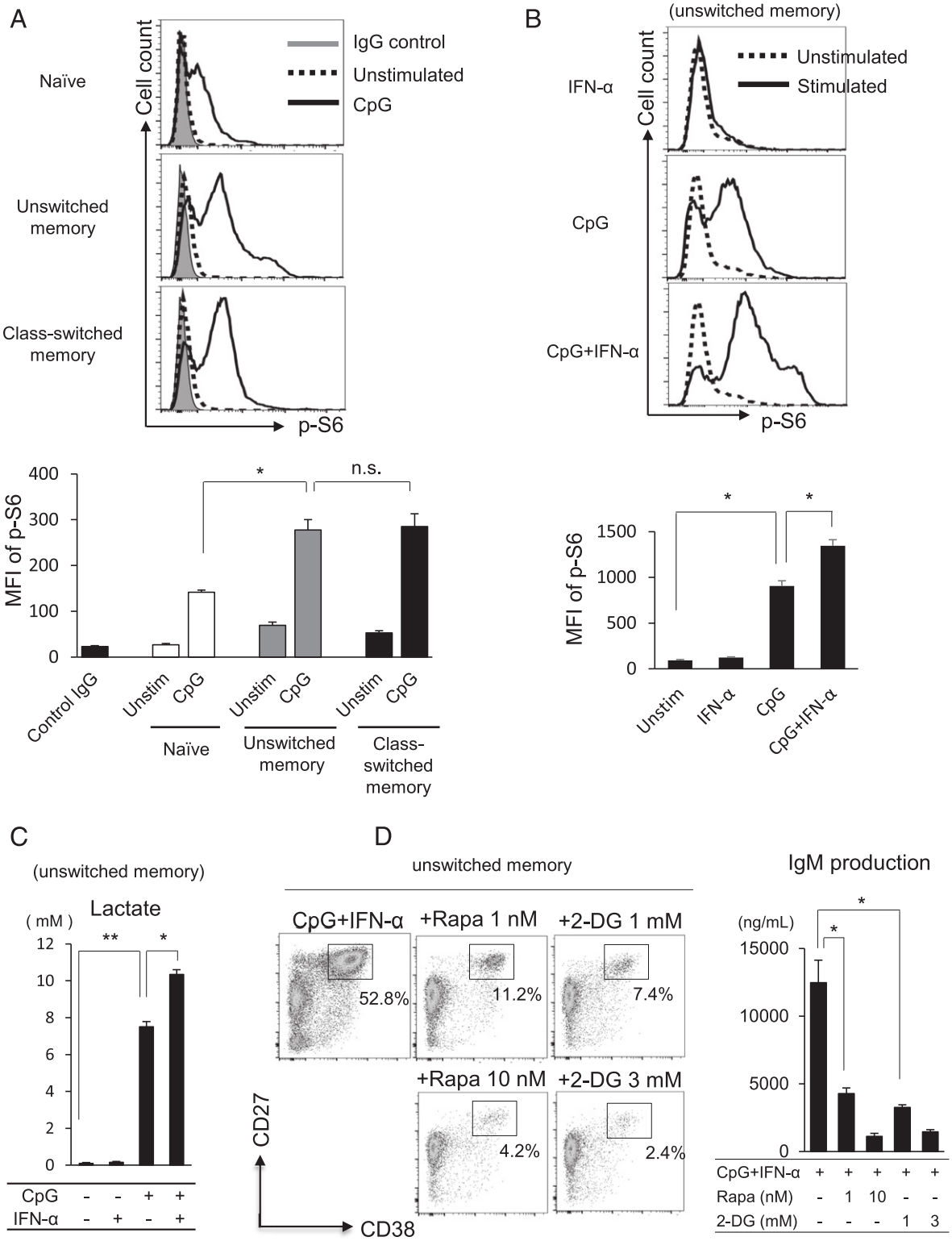

FIGURE 4. CpG and IFN-α enhanced mTORC1 activation and glycolysis, leading to plasmablast differentiation into human $CD27^+IgD^+$ unswitched memory B cells. (**A**) p-S6 (s235/236 site) in B cell subsets was analyzed by intracellular staining after a 5-d culture. (**B**) $CD27^+IgD^+$ unswitched memory B cells were cultured with IFN-α and/or CpG for 5 d, and p-S6 was analyzed by intracellular staining. (**C**) Culture medium from $CD27^+IgD^+$ unswitched memory B cells was collected on day 5 and analyzed for lactate production, a sensitive readout of glycolysis, using a colorimetric assay kit. (**D**) $CD27^+IgD^+$ unswitched memory B cells were cultured with CpG and IFN-α in the presence of rapamycin or 2-DG. The percentage of $CD27^{hi}CD38^{hi}$ plasmablasts was determined by flow cytometry, and IgM production was assessed by ELISA. Dot plots and bar graphs are representative of three or more independent experiments that yielded the same results. Data are mean ± SEM of three experiments using cells from three donors. $*p < 0.05$, $**p < 0.01$.

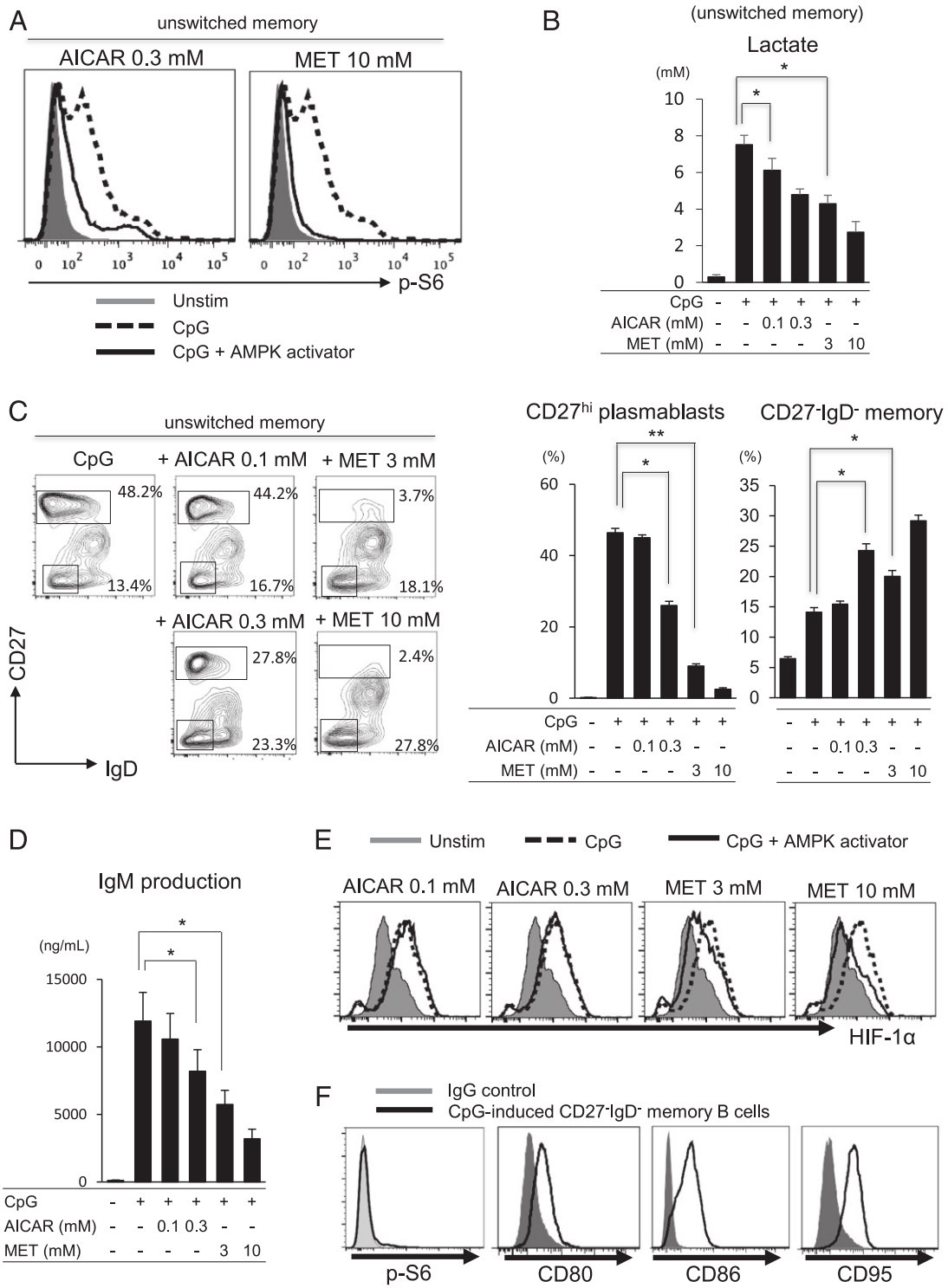

FIGURE 5. AMPK activation prevented $CD27^+IgD^+$ unswitched memory B cell–plasmablast differentiation but supported $CD27^-IgD^-$ B cell transition. $CD27^+IgD^+$ unswitched memory B cells were harvested and analyzed after a 5-d stimulation and treatment. (**A**) The cells were analyzed by flow cytometry for p-S6. (**B**) Lactate concentration. (**C**) Percentages of plasmablasts and $CD27^-IgD^-$ B cells of $CD27^+IgD^+$ unswitched memory B cell origin. (**D**) IgM production. (**E**) Expression of HIF-1α in $CD27^+IgD^+$ unswitched memory B cells. (**F**) Expression levels of p-S6, CD80, CD86, and CD95 in CpG-induced $CD27^-IgD^-$ B cells were analyzed by flow cytometry. Contour plots and graphs are representative of three independent experiments that yielded the same results. Data are mean ± SEM of three experiments using cells from three donors. $*p < 0.05$, $**p < 0.01$. MET, metformin.

B cells to $CD27^-IgD^-$ B cells, but it suppressed mTORC1 activation, lactate production, and differentiation into plasmablasts.

$CD19^+$ B cells are considered a heterogeneous population that includes effector and memory phenotypes. We (3) and other investigators (30, 35) have reported that $CD27^+$ memory B cells carry higher potentials for inflammatory responses do than $CD27^-$ naive B cells. However, to our knowledge, this is the first study that thoroughly elucidated and compared the differentiation of $CD27^-IgD^+$ naive B cells, $CD27^+IgD^+$ unswitched memory B cells, and $CD27^+IgD^-$ class-switched memory B cells, with a special focus on the metabolic pathway. Namely, the addition of IFN-α and CpG/TLR9 to unswitched memory B cells increased the secretion of

Table I. Clinical characteristics of SLE patients and healthy subjects

Characteristic	SLE (n = 48)	Control (n = 16)
Age (y; mean [range])	40.6 (18–69)	29.3 (21–47)
Sex (women/men)	43/5	15/1
Disease duration (mo; mean [range])	142.4 (1–432)	
Medications (n)		
No treatment	8	
Corticosteroids	28	
Cyclophosphamide	13	
Mycophenolate mofetil	1	
Tacrolimus	9	
Cyclosporine A	7	
Hydroxychloroquine	4	
Azathioprine	7	
Mizoribine	6	
Methotrexate	5	
Anti-dsDNA Ab (IU/ml; mean ± SD)	45.6 ± 87.9	
CH50 (U/ml; mean ± SD)	40.5 ± 17.9	
SLEDAI score (range)	10.3 (0–33)	
BILAG score (range)	11.4 (0–45)	

BILAG, British Isles Lupus Assessment Group disease activity index; CH50, 50% hemolytic complement activity; SLEDAI, SLE disease activity index.

IgM, IL-6, and TNF-α. These findings are consistent with previous reports that highlighted the importance of unswitched memory B cells in the first-line defense against infections through rapid and predominant production of low-affinity, but high-avidity, IgM (13, 14). In contrast, the combination of CpG and IFN-α induced the production of IL-10, but not IgG or IgM from naive B cells. Menon et al. (36) and other investigators (37) also demonstrated the IL-10–producing capacity of naive B cells under similar stimulatory conditions, defining them as regulatory B cells. Thus, it seems that a delicate balance in the functions of different B cell subsets that are induced by different stimuli plays a critical role in immune homeostasis.

Recent studies have demonstrated that cellular metabolism regulates the functions and differentiation of lymphocytes (38). With regard to $CD4^+$ and $CD8^+$ naive T cells, the TCR signal enhances mTORC1 activity and glycolysis, triggering anabolic switch. This metabolic process enhances vigorous proliferation and facilitates differentiation into effector T cells (20, 21, 39–41). However, the cellular metabolism in human B cell subsets has been studied minimally. We demonstrated in the current study that CpG/TLR9 and IFN-α synergistically induced mTORC1 activation and glycolysis, and these metabolic changes proved important for the differentiation of unswitched memory B cells to plasmablasts (Fig. 4). B cells show accelerated cell division and increased cell size during the process of plasmablast differentiation (30), then, in turn, plasmablasts secrete plenty of Ig. We also demonstrated that inhibition of the mTORC1–glycolysis pathway with rapamycin, 2-DG, AICAR, and metformin attenuated the robust proliferation of $CD27^+IgD^+$ unswitched memory B cells, as well as plasmablast differentiation (Supplemental Fig. 3C). Therefore, our findings on B cell metabolism suggest that differentiation into plasmablasts requires large amounts of nutrients and energy through the anabolic glycolysis system.

Our results demonstrated that the CpG/TLR9 signal can induce the transformation of unswitched memory B cells to functional $CD27^-IgD^-$ B cells expressing high levels of costimulatory molecules and activation marker (Fig. 5F). We also examined the effect of loxoribine, a synthetic TLR7 ligand that is closely involved in the pathogenesis of SLE (42) and in the differentiation of unswitched memory B cells. The combination of loxoribine and IFN-α induced plasmablast differentiation, whereas loxoribine alone, unlike CpG, did not induce $CD27^-IgD^-$ B cells from unswitched memory B cells (Supplemental Fig. 1D). These results suggest that induction of $CD27^-IgD^-$ B cells is specific to the TLR9 signal.

$CD27^-IgD^-$ B cells account for <5% of peripheral blood B cells in healthy subjects (43), but this population can increase in certain viral infections and active SLE. They are considered to act as an immune memory subset prepared for future Ag re-exposure and contribute to pathogen removal or exacerbation of SLE (43–46). The expanded $CD27^-IgD^-$ B cells in SLE express high levels of CD95 (45, 47). In our study, CpG induced CD95-expressing $CD27^-IgD^-$ B cells from unswitched memory B cells (Fig. 5F). These results indicate that CpG-stimulated unswitched memory B cells could be the source of $CD27^-IgD^-$ B cells in patients with SLE. It is noteworthy that the AMPK pathway enhanced $CD27^-IgD^-$ B cell development from unswitched memory B cells, whereas it suppressed the mTORC1–glycolysis pathway and inhibited plasmablast differentiation. More importantly, CpG-induced $CD27^-IgD^-$ B cells did not show mTORC1 activation (Fig. 5F). In addition, inhibition of mTORC1 only did not induce this population (Supplemental Fig. 3D). Collectively, these results indicate that AMPK activation is important for $CD27^-IgD^-$ B cell induction. Several studies reported that such a change in the metabolic pattern, including AMPK and its downstream oxidative phosphorylation, induces differentiation of memory $CD8^+$ T cells (25, 48, 49). Lam et al. (50) reported that long-term survival of long-lived plasma cells depends on a shift to oxidative phosphorylation. Just like memory B cells, long-lived plasma cells remain functional over several years. This longevity is necessary to maintain immunological memory and to prevent reinfection. Quiescent and slow, but efficient, ATP generation through AMPK signaling and mitochondrial oxidative phosphorylation may be advantageous for long living B-lineage cells. Although the cell types and species are different, our study provides further support for the findings from the above studies. It is presumed that activation of AMPK and its downstream oxidative phosphorylation contribute to development of the $CD27^-IgD^-$ population. However, a limitation of our study was the fact that we were unable to evaluate the detailed mechanism of AMPK in unswitched memory B cells, because of the small number of this subset obtained from the peripheral blood of healthy donors. Thus, the balance between mTORC1–glycolysis and AMPK appears to commit the differentiation of unswitched memory B cells to plasmablasts and $CD27^-IgD^-$ B cells, respectively, and any imbalance may commit to pathological processes, such as SLE, whereby mTORC1 activation in $CD19^+$ B cells was closely related to plasmablast differentiation and disease activity (Fig. 6).

mTORC1 activation has been reported in murine B cells (51) and in T cells of SLE (52). In addition, rapamycin and metformin are reported to improve disease severity in murine lupus models (51, 53). In patients with active SLE, Ag stimulation of TLRs, BCRs and TCRs, and various inflammatory mediators, such as cytokines, including IFNs, are abundant and activate lymphocytes (54). mTORC1 phosphorylation can be induced by the TLR9 signal and IFN-α in B cells, whereas it is induced by TCR stimulation and SLE-relevant cytokines in T cells (55). Our study investigated for the first time, to our knowledge, the correlation between mTORC1 activation in peripheral B cells and the clinical background of patients with SLE. Our results emphasize the potential therapeutic benefits of mTORC1 inhibition in T and B cells in SLE.

In the fields of oncology, organ transplantation, allergy, and autoimmune diseases, cellular metabolism, including the

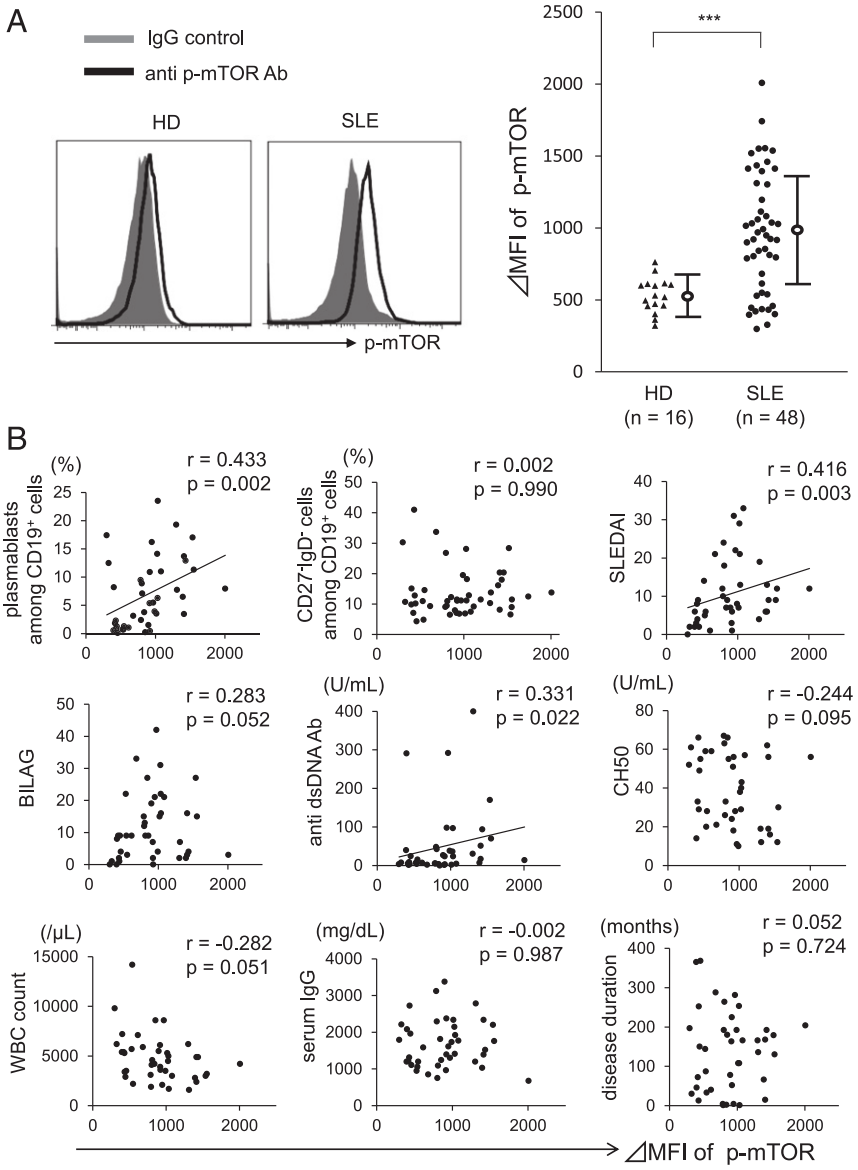

FIGURE 6. mTOR phosphorylation in B cells is closely related to the pathogenesis of SLE. PBMCs were obtained from 16 healthy donors and 48 SLE patients, and $CD19^+$ B cells were gated, excluding $CD27^{hi}CD38^{hi}$ plasmablasts. (**A**) p-mTOR in $CD19^+$ B cells of healthy subjects (HD) and patients with SLE was analyzed by flow cytometry and is shown in the representative line graphs (left panel) and scatter plots (right panel). ΔMFI represents the difference in MFI between the samples and IgG control. Data are mean ± SD. (**B**) Correlation between p-mTOR levels and clinical background. Correlations were assessed using the Spearman rank correlation coefficient. ***$p < 0.001$, Student *t* test.

mTORC1–glycolysis and AMPK pathways, is gathering attention as a potential therapeutic target, and certain therapeutic agents based on this concept are already being tested clinically (20, 56–61). Our findings highly suggest the involvement of CpG/TLR9 and IFN-α in the differentiation of unswitched memory B cells, through the differential pathway of metabolic reprogramming, into plasmablasts (CpG and IFN-α–mTORC1 pathway) or $CD27^-IgD^-$ memory B cells (CpG alone–AMPK pathway), which could aid in the development of new therapies for various immune disorders.

Acknowledgments

We thank the patients and healthy subjects for their cooperation and for consenting to participate in the study.

Disclosures

K.S. is an employee of Mitsubishi Tanabe Pharma. Y.T. received research grants from Mitsubishi-Tanabe, Takeda, Daiichi-Sankyo, Chugai, Bristol-Myers, MSD, Astellas, Abbvie, and Eisai. H.S. received research grants from MSD, Bayer, Taisho-Toyama, Daiichi-Sankyo, Lilly, Dainippon-Sumitomo, Ono, Mochida, Boehringer Ingelheim, and Chugai pharmaceuticals. The other authors have no financial conflicts of interest.

References

1. Hornung, V., S. Rothenfusser, S. Britsch, A. Krug, B. Jahrsdörfer, T. Giese, S. Endres, and G. Hartmann. 2002. Quantitative expression of toll-like receptor 1-10 mRNA in cellular subsets of human peripheral blood mononuclear cells and sensitivity to CpG oligodeoxynucleotides. *J. Immunol.* 168: 4531–4537.
2. Poeck, H., M. Wagner, J. Battiany, S. Rothenfusser, D. Wellisch, V. Hornung, B. Jahrsdorfer, T. Giese, S. Endres, and G. Hartmann. 2004. Plasmacytoid dendritic cells, antigen, and CpG-C license human B cells for plasma cell differentiation and immunoglobulin production in the absence of T-cell help. *Blood* 103: 3058–3064.
3. Iwata, S., K. Yamaoka, H. Niiro, K. Nakano, S.-P. Wang, K. Akashi, and Y. Tanaka. 2012. Amplification of Toll-like receptor-mediated signaling through spleen tyrosine kinase in human B-cell activation. *J. Allergy Clin. Immunol.* 129: 1594–601.e2.
4. Brummel, R., and P. Lenert. 2005. Activation of marginal zone B cells from lupus mice with type A(D) CpG-oligodeoxynucleotides. *J. Immunol.* 174: 2429–2434.
5. Iwata, S., and Y. Tanaka. 2016. B-cell subsets, signaling and their roles in secretion of autoantibodies. *Lupus* 25: 850–856.
6. Liu, Y. J. 2001. Dendritic cell subsets and lineages, and their functions in innate and adaptive immunity. *Cell* 106: 259–262.
7. Le Bon, A., G. Schiavoni, G. D'Agostino, I. Gresser, F. Belardelli, and D. F. Tough. 2001. Type I interferons potently enhance humoral immunity and can promote isotype switching by stimulating dendritic cells in vivo. *Immunity* 14: 461–470.
8. Ruuth, K., L. Carlsson, B. Hallberg, and E. Lundgren. 2001. Interferon-alpha promotes survival of human primary B-lymphocytes via phosphatidylinositol 3-kinase. *Biochem. Biophys. Res. Commun.* 284: 583–586.
9. Leadbetter, E. A., I. R. Rifkin, A. M. Hohlbaum, B. C. Beaudette, M. J. Shlomchik, and A. Marshak-Rothstein. 2002. Chromatin-IgG complexes activate B cells by dual engagement of IgM and Toll-like receptors. *Nature* 416: 603–607.

10. Weller, S., A. Faili, C. Garcia, M. C. Braun, F. F. Le Deist, G. G. de Saint Basile, O. Hermine, A. Fischer, C. A. Reynaud, and J. C. Weill. 2001. CD40-CD40L independent Ig gene hypermutation suggests a second B cell diversification pathway in humans. *Proc. Natl. Acad. Sci. USA* 98: 1166–1170.
11. Kruetzmann, S., M. M. Rosado, H. Weber, U. Germing, O. Tournilhac, H.-H. Peter, R. Berner, A. Peters, T. Boehm, A. Plebani, et al. 2003. Human immunoglobulin M memory B cells controlling *Streptococcus pneumoniae* infections are generated in the spleen. *J. Exp. Med.* 197: 939–945.
12. Weller, S., M. C. Braun, B. K. Tan, A. Rosenwald, C. Cordier, M. E. Conley, A. Plebani, D. S. Kumararatne, D. Bonnet, O. Tournilhac, et al. 2004. Human blood IgM "memory" B cells are circulating splenic marginal zone B cells harboring a prediversified immunoglobulin repertoire. *Blood* 104: 3647–3654.
13. Capolunghi, F., S. Cascioli, E. Giorda, M. M. Rosado, A. Plebani, C. Auriti, G. Seganti, R. Zuntini, S. Ferrari, M. Cagliuso, et al. 2008. CpG drives human transitional B cells to terminal differentiation and production of natural antibodies. *J. Immunol.* 180: 800–808.
14. Carsetti, R., M. M. Rosado, S. Donnanno, V. Guazzi, A. Soresina, A. Meini, A. Plebani, F. Aiuti, and I. Quinti. 2005. The loss of IgM memory B cells correlates with clinical disease in common variable immunodeficiency. *J. Allergy Clin. Immunol.* 115: 412–417.
15. Kurosaki, T., K. Kometani, and W. Ise. 2015. Memory B cells. *Nat. Rev. Immunol.* 15: 149–159.
16. Kaech, S. M., and W. Cui. 2012. Transcriptional control of effector and memory CD8+ T cell differentiation. *Nat. Rev. Immunol.* 12: 749–761.
17. O'Neill, L. A., and E. J. Pearce. 2016. Immunometabolism governs dendritic cell and macrophage function. *J. Exp. Med.* 213: 15–23.
18. Finlay, D. K. 2015. Metabolic regulation of natural killer cells. *Biochem. Soc. Trans.* 43: 758–762.
19. Buck, M. D., D. O'Sullivan, and E. L. Pearce. 2015. T cell metabolism drives immunity. *J. Exp. Med.* 212: 1345–1360.
20. Sukumar, M., J. Liu, Y. Ji, M. Subramanian, J. G. Crompton, Z. Yu, R. Roychoudhuri, D. C. Palmer, P. Muranski, E. D. Karoly, et al. 2013. Inhibiting glycolytic metabolism enhances CD8+ T cell memory and antitumor function. *J. Clin. Invest.* 123: 4479–4488.
21. Delgoffe, G. M., K. N. Pollizzi, A. T. Waickman, E. Heikamp, D. J. Meyers, M. R. Horton, B. Xiao, P. F. Worley, and J. D. Powell. 2011. The kinase mTOR regulates the differentiation of helper T cells through the selective activation of signaling by mTORC1 and mTORC2. *Nat. Immunol.* 12: 295–303.
22. Laplante, M., and D. M. Sabatini. 2012. mTOR signaling in growth control and disease. *Cell* 149: 274–293.
23. Dibble, C. C., and B. D. Manning. 2013. Signal integration by mTORC1 coordinates nutrient input with biosynthetic output. *Nat. Cell Biol.* 15: 555–564.
24. van der Windt, G. J., and E. L. Pearce. 2012. Metabolic switching and fuel choice during T-cell differentiation and memory development. *Immunol. Rev.* 249: 27–42.
25. Rolf, J., M. Zarrouk, D. K. Finlay, M. Foretz, B. Viollet, and D. A. Cantrell. 2013. AMPKα1: a glucose sensor that controls CD8 T-cell memory. *Eur. J. Immunol.* 43: 889–896.
26. Benhamron, S., S. P. Pattanayak, M. Berger, and B. Tirosh. 2015. mTOR activation promotes plasma cell differentiation and bypasses XBP-1 for immunoglobulin secretion. *Mol. Cell. Biol.* 35: 153–166.
27. Jellusova, J., and R. C. Rickert. 2016. The PI3K pathway in B cell metabolism. *Crit. Rev. Biochem. Mol. Biol.* 51: 359–378.
28. Brink, R., C. C. Goodnow, J. Crosbie, E. Adams, J. Eris, D. Y. Mason, S. B. Hartley, and A. Basten. 1992. Immunoglobulin M and D antigen receptors are both capable of mediating B lymphocyte activation, deletion, or anergy after interaction with specific antigen. *J. Exp. Med.* 176: 991–1005.
29. Pone, E. J., J. Zhang, T. Mai, C. A. White, G. Li, J. K. Sakakura, P. J. Patel, A. Al-Qahtani, H. Zan, Z. Xu, and P. Casali. 2012. BCR-signalling synergizes with TLR-signalling for induction of AID and immunoglobulin class-switching through the non-canonical NF-κB pathway. *Nat. Commun.* 3: 767.
30. Tangye, S. G., D. T. Avery, and P. D. Hodgkin. 2003. A division-linked mechanism for the rapid generation of Ig-secreting cells from human memory B cells. *J. Immunol.* 170: 261–269.
31. Foretz, M., S. Hébrard, J. Leclerc, E. Zarrinpashneh, M. Soty, G. Mithieux, K. Sakamoto, F. Andreelli, and B. Viollet. 2010. Metformin inhibits hepatic gluconeogenesis in mice independently of the LKB1/AMPK pathway via a decrease in hepatic energy state. *J. Clin. Invest.* 120: 2355–2369.
32. Corton, J. M., J. G. Gillespie, S. A. Hawley, and D. G. Hardie. 1995. 5-aminoimidazole-4-carboxamide ribonucleoside. A specific method for activating AMP-activated protein kinase in intact cells? *Eur. J. Biochem.* 229: 558–565.
33. Harris, A. L. 2002. Hypoxia–a key regulatory factor in tumour growth. *Nat. Rev. Cancer* 2: 38–47.
34. Rosner, M., N. Siegel, A. Valli, C. Fuchs, and M. Hengstschläger. 2010. mTOR phosphorylated at S2448 binds to raptor and rictor. *Amino Acids* 38: 223–228.
35. Tangye, S. G., D. T. Avery, E. K. Deenick, and P. D. Hodgkin. 2003. Intrinsic differences in the proliferation of naive and memory human B cells as a mechanism for enhanced secondary immune responses. *J. Immunol.* 170: 686–694.
36. Menon, M., P. A. Blair, D. A. Isenberg, and C. Mauri. 2016. A regulatory feedback between plasmacytoid dendritic cells and regulatory B cells is aberrant in systemic lupus erythematosus. *Immunity* 44: 683–697.
37. Matsumoto, M., A. Baba, T. Yokota, H. Nishikawa, Y. Ohkawa, H. Kayama, A. Kallies, S. L. Nutt, S. Sakaguchi, K. Takeda, et al. 2014. Interleukin-10-producing plasmablasts exert regulatory function in autoimmune inflammation. *Immunity* 41: 1040–1051.
38. Pearce, E. L., M. C. Poffenberger, C.-H. Chang, and R. G. Jones. 2013. Fueling immunity: insights into metabolism and lymphocyte function. *Science* 342: 1242454.
39. Michalek, R. D., V. A. Gerriets, S. R. Jacobs, A. N. Macintyre, N. J. MacIver, E. F. Mason, S. A. Sullivan, A. G. Nichols, and J. C. Rathmell. 2011. Cutting edge: distinct glycolytic and lipid oxidative metabolic programs are essential for effector and regulatory CD4+ T cell subsets. *J. Immunol.* 186: 3299–3303.
40. Chang, J. T., E. J. Wherry, and A. W. Goldrath. 2014. Molecular regulation of effector and memory T cell differentiation. *Nat. Immunol.* 15: 1104–1115.
41. Yang, K., S. Shrestha, H. Zeng, P. W. Karmaus, G. Neale, P. Vogel, D. A. Guertin, R. F. Lamb, and H. Chi. 2013. T cell exit from quiescence and differentiation into Th2 cells depend on Raptor-mTORC1-mediated metabolic reprogramming. *Immunity* 39: 1043–1056.
42. Marshak-Rothstein, A. 2006. Toll-like receptors in systemic autoimmune disease. *Nat. Rev. Immunol.* 6: 823–835.
43. Wei, C., J. Anolik, A. Cappione, B. Zheng, A. Pugh-Bernard, J. Brooks, E.-H. Lee, E. C. B. Milner, and I. Sanz. 2007. A new population of cells lacking expression of CD27 represents a notable component of the B cell memory compartment in systemic lupus erythematosus. *J. Immunol.* 178: 6624–6633.
44. Sanz, I., C. Wei, F. E.-H. Lee, and J. Anolik. 2008. Phenotypic and functional heterogeneity of human memory B cells. *Semin. Immunol.* 20: 67–82.
45. Jacobi, A. M., K. Reiter, M. Mackay, C. Aranow, F. Hiepe, A. Radbruch, A. Hansen, G.-R. Burmester, B. Diamond, P. E. Lipsky, and T. Dörner. 2008. Activated memory B cell subsets correlate with disease activity in systemic lupus erythematosus: delineation by expression of CD27, IgD, and CD95. *Arthritis Rheum.* 58: 1762–1773.
46. Wirths, S., and A. Lanzavecchia. 2005. ABCB1 transporter discriminates human resting naive B cells from cycling transitional and memory B cells. *Eur. J. Immunol.* 35: 3433–3441.
47. Rodríguez-Bayona, B., A. Ramos-Amaya, J. J. Pérez-Venegas, C. Rodríguez, and J. A. Brieva. 2010. Decreased frequency and activated phenotype of blood CD27 IgD IgM B lymphocytes is a permanent abnormality in systemic lupus erythematosus patients. *Arthritis Res. Ther.* 12: R108.
48. Araki, K., and R. Ahmed. 2013. AMPK: a metabolic switch for CD8+ T-cell memory. *Eur. J. Immunol.* 43: 878–881.
49. Yang, K., and H. Chi. 2015. AMPK helps T cells survive nutrient starvation. *Immunity* 42: 4–6.
50. Lam, W. Y., A. M. Becker, K. M. Kennerly, R. Wong, J. D. Curtis, E. M. Llufrio, K. S. McCommis, J. Fahrmann, H. A. Pizzato, R. M. Nunley, et al. 2016. Mitochondrial pyruvate import promotes long-term survival of antibody-secreting plasma cells. *Immunity* 45: 60–73.
51. Wu, T., X. Qin, Z. Kurepa, K. R. Kumar, K. Liu, H. Kanta, X. J. Zhou, A. B. Satterthwaite, L. S. Davis, and C. Mohan. 2007. Shared signaling networks active in B cells isolated from genetically distinct mouse models of lupus. *J. Clin. Invest.* 117: 2186–2196.
52. Fernandez, D. R., T. Telarico, E. Bonilla, Q. Li, S. Banerjee, F. A. Middleton, P. E. Phillips, M. K. Crow, S. Oess, W. Muller-Esterl, and A. Perl. 2009. Activation of mammalian target of rapamycin controls the loss of TCRzeta in lupus T cells through HRES-1/Rab4-regulated lysosomal degradation. *J. Immunol.* 182: 2063–2073.
53. Yin, Y., S.-C. Choi, Z. Xu, L. Zeumer, N. Kanda, B. P. Croker, and L. Morel. 2016. Glucose oxidation is critical for CD4+ T cell activation in a mouse model of systemic lupus erythematosus. *J. Immunol.* 196: 80–90.
54. Pathak, S., and C. Mohan. 2011. Cellular and molecular pathogenesis of systemic lupus erythematosus: lessons from animal models. *Arthritis Res. Ther.* 13: 241.
55. Pollizzi, K. N., and J. D. Powell. 2015. Regulation of T cells by mTOR: the known knowns and the known unknowns. *Trends Immunol.* 36: 13–20.
56. Perl, A. 2016. Activation of mTOR (mechanistic target of rapamycin) in rheumatic diseases. *Nat. Rev. Rheumatol.* 12: 169–182.
57. Long, J.-P., X.-N. Li, and F. Zhang. 2016. Targeting metabolism in breast cancer: how far we can go? *World J. Clin. Oncol.* 7: 122–130.
58. Lee, J. J., K. Loh, and Y.-S. Yap. 2015. PI3K/Akt/mTOR inhibitors in breast cancer. *Cancer Biol. Med.* 12: 342–354.
59. Gurk-Turner, C., W. Manitpisitkul, and M. Cooper. 2012. A comprehensive review of everolimus clinical reports: a new mammalian target of rapamycin inhibitor. *Transplantation* 94: 659–668.
60. Huang, Q., and R. M. Pope. 2010. Toll-like receptor signaling: a potential link among rheumatoid arthritis, systemic lupus, and atherosclerosis. *J. Leukoc. Biol.* 88: 253–262.
61. Yap, M., S. Brouard, C. Pecqueur, and N. Degauque. 2015. Targeting CD8 T-cell metabolism in transplantation. *Front. Immunol.* 6: 547.